JOURNAL OF Materials CHEMISTRY

Synthesis of novel inorganic structures under unusual high pressure gas and hydrothermal conditions†

Mark T. Weller,*[a] Sandra E. Dann,[b] Paul F. Henry[a] and David B. Currie[a]

[a]*Department of Chemistry, University of Southampton, Highfield, Southampton, UK SO17 1BJ. E-mail: mtw@soton.ac.uk*
[b]*Department of Chemistry, University of Loughborough, Loughborough, UK LE11 3TU*

Received 21st April 1998, Accepted 18th June 1998

The application of high pressures to synthesis in inorganic materials chemistry significantly widens the range and type of compound that can be prepared. Three different high pressure systems that allow, respectively, synthesis under flowing oxygen, nitrogen and hydrothermal conditions are described together with a new result obtained on each. Under hydrothermal conditions a framework material of the composition $Ca_8[AlGaSiO_6]_4(OH)_8$ has been prepared and structural analysis shows that this material contains uniquely linkages of the type Al–O–Ga. Under high pressure nitrogen, copper has been doped into the Li_3N structure to levels higher than previously achieved and with high pressure oxygen a series of new phases of the type $Ln_2Ba_4Cu_{7-x}Ni_xO_{14+\delta}$ (247) (Ln = lanthanide, yttrium) have been synthesised. The valuable role of high pressures in synthetic solid state chemistry is discussed.

Much synthetic work in materials chemistry has followed the traditional route of direct reaction of simple phases under high temperature, ambient pressure conditions. While this method continues to produce a wealth of new materials, it limits developments and the type of phase that can be synthesised for many reasons. For example, under ambient pressures volatile components evaporate and are lost from the reaction mixture and low stability complex anions frequently decompose to oxide, while under high pressures materials derived from volatile heavy B metal oxides and carbonate can be formed readily. Thus materials such as the superconducting phases $HgBa_2Ca_5Cu_6O_{13+\delta}$ and $(Cu,C)Ba_2Ca_3Cu_4O_{11+\delta}$ may be synthesised under pressures over 50 kbar.[1] An additional factor is that, to some extent, phase stability can be changed through application of pressure, for example denser, high co-ordination structures are generally preferred. A well known example of this behaviour is the formation of six co-ordinate silicon in $MgSiO_3$ at 250 kbar.[2]

Synthesis under high pressure can be accomplished in a number of ways, for example through increased gas pressure, externally or internally generated hydrothermal pressure or through hydrostatic pressure using devices such as solid state presses. The major proportion of syntheses carried out under high pressures has involved apparatus which generates the pressure using belt or anvil devices. Such systems, though widely used, have a number of problems due to restricted sample size, pressure inhomogeneity and poor control of the reaction atmosphere; for example oxygen may only be generated under these conditions through uncontrolled decomposition reactions. Some other high-pressure systems use sealed vessels in combination with gas cylinder pressures with limitations on the maximum pressure and temperature.[3,4]

In this paper we describe three systems used for synthesising moderate quantities of inorganic materials under high pressures up to 4 kbar. These systems vary depending on the systems to be investigated.

Experimental

Apparatus for synthesis under high pressure

A system which uses flowing oxygen at pressure up to 1 kbar and at temperatures to 1100 °C has been described previously.[5] The apparatus uses a double vessel system, with an inner alumina tube containing a small volume of oxygen under high pressure, surrounded by a Nimonic steel pressure vessel containing high pressure nitrogen, with a governor balancing the pressure between the two (Fig. 1). The oxygen pressure, delivered by a compressor, is set at a value slightly higher than that of the surrounding nitrogen allowing a continuous flow of oxygen over the sample. This continuous replacement of the oxygen is a feature not accessible with many other systems for reaction under high-pressure oxygen, where a closed vessel is heated. The apparatus has been widely used to study the formation of highly oxidised transition metals, particularly those of the late first row transition series.[6–8]

Synthesis under high-pressure nitrogen was undertaken using a simpler, single pressure vessel system and an external furnace. One feature of nitride synthesis under high pressure is that the reactants and products may be extremely water and oxygen sensitive. With high pressures a low proportion of contaminant oxygen can still represent a significant amount resulting in rapid oxidation of notable quantities of material. The system used in this work consisted of a short Nimonic steel pressure vessel, which was sealed and taken complete in and out of a glove box. The pressure vessel was loaded with the reaction mixture in an atmosphere containing less than 1 ppm of oxygen and moisture, sealed and then transferred to the high-pressure line. Electronic grade nitrogen was compressed to 200 bar and the couplings to the pressure vessel flushed with this gas several times. The vessel was then filled and heated to the reaction temperature using an external furnace. After reaction the furnace was cooled and the pressure discharged from the vessel before it was transferred complete to the glove box.

The high-pressure hydrothermal apparatus was based on the cold-seal Tuttle type and the complete system is shown schematically in Fig. 2. The apparatus was surrounded by an 8 mm steel cabinet and the volume of water under pressure minimised by using a filler rod to reduce the bomb volume and therefore reduce the potential hazards associated with the experiment. A safety reservoir was also used to balance any pressure changes in the bomb, which was constructed from Rene-77 alloy (high Ni). In a typical experiment the reactants were mixed thoroughly, solvent added using a microsyringe and then sealed, by arc-welding, in a thick walled gold capsule. The capsule was then weighed, placed in the bomb and a filler

†Basis of the presentation given at Materials Chemistry Discussion No. 1, 24–26 September 1998, ICMCB, University of Bordeaux, France.

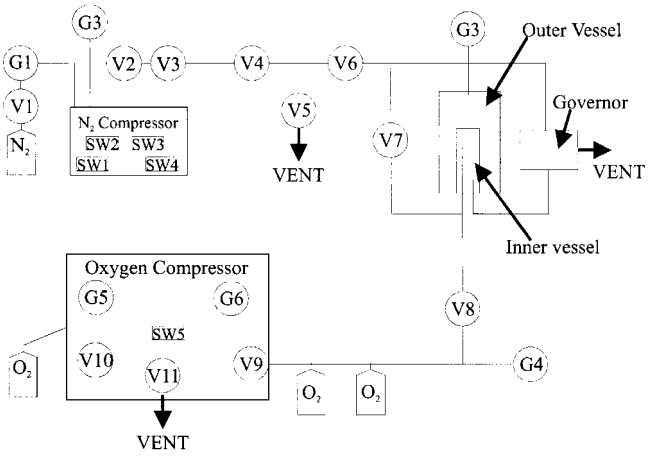

Fig. 1 Schematic diagram of the high-pressure oxygen rig showing connections to the double volume pressure vessel.

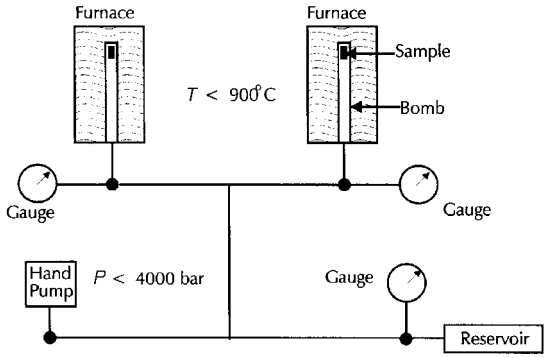

Fig. 2 Schematic diagram of the hydrothermal apparatus.

rod added on top; water was then be used to fill the rest of the space (*ca.* 1–2 ml). The bomb was sealed by deformation of a high-pressure end cone. Two thermocouples were used, one to control the furnace temperature and the second to monitor the sample temperature. The furnace was then lowered over the bomb and the bomb opened to the line *via* a three-way offset cross valve. This valve was essential as it allowed the pressure in the bomb to be monitored constantly *via* a gauge. The reservoir (1 l kept at 1 kbar) was then opened and the furnace then switched on. Once the furnace reached its operating temperature the pump was used to top up the pressure after the reservoir had been closed off. The three way valve was then closed and the experiment proceeded for the reaction period. Finally the furnace was switched off and the bomb allowed to cool; once the pressure reached 1 kbar the connection to the reservoir was opened again and the system left to reach room temperature. After cooling the bomb was opened, the capsule removed and weighed to ensure sample integrity.

Systems synthesised

Synthesis of aluminium gallium bicchulite. Bicchulite $Ca_8[Al_2SiO_6]_4(OH)_8$ is a rare mineral with a structure based on that of sodalite.[9] The framework consists of directly linked β-cages containing a cubic $Ca_4(OH)_4$ unit with hydroxide and calcium ions at alternating corners. One unusual feature of this framework is the presence of Al–O–Al linkages not found in other aluminosilicate frameworks. We have recently reported the synthesis of a gallium analogue of this material, $Ca_8[Ga_2SiO_6]_4(OH)_8$,[10,11] where the framework contains novel, directly linked GaO_4 tetrahedra, which are locally ordered in structural domains similar to those in tugtupite.[12] No structure has been described previously containing Ga–O–Al links but in this article we report the synthesis of $Ca_8[AlGaSiO_6]_4(OH)_8$ with a framework containing this unique feature.

$Ca_8[AlGaSiO_6]_4(OH)_8$ was synthesised by reaction of a previously prepared gehlenite type material $Ca_2GaAlSiO_7$ (2 g) with 0.5 ml of water in a sealed gold tube at 540 °C, under 1 kbar hydrothermal pressure for two days. The product was structurally characterised by powder X-ray and neutron diffraction. Powder X-ray diffraction data were collected on a Siemens D5000 diffractometer, operating with Cu-Kα_1 radiation, in the 2θ range 10–110° with a step size of 0.02°, over a period of 15 h. Powder neutron diffraction data were collected on D2B, ILL Grenoble, operating with a wavelength of 1.59 Å, over a period of 8 h. Profile refinement of the gallium aluminium bicchulite structure was initially undertaken using the powder X-ray diffraction data, but owing to the insensitivity of this technique to the light atom positions a higher quality refinement could be achieved with the neutron diffraction data. For this reason only the results from the neutron work are presented here. The initial starting model was taken from that of bicchulite using a disordered framework but with equal amounts of gallium, aluminium and silicon occupying the tetrahedral sites. Hydrogen was placed on a one-third occupied (*xxz*) site, as it had been previously for this structure type. The GSAS refinement[13] converged smoothly to give the final atomic parameters summarised in Table 1, derived bond distances and lengths are given in Table 2. The final fit achieved to the profile is shown in Fig. 3 and the structure is shown in Fig. 4. The structural parameters are as expected for a material adopting the bicchulite structure with a cube of the stoichiometry $Ca_4(OH)_4$ at the centre of the sodalite cage. Perhaps

Table 1 Final refined atomic parameters for $Ca_8[AlGaSiO_6]_4(OH)_8$ [$a = 8.88114(6)$ Å, space group $I\bar{4}3m$]

Atom	x	y	z	$U_{iso} \times 100/Å^2$
Ga/Si/Al	0.25	0.5	0	0.80(8)
O	0.1401(2)	0.1401(2)	0.4180(2)	1.47(3)
Ca	0.1426(3)	0.1426(3)	0.1426(3)	1.65(5)
O	0.3830(2)	0.3830(2)	0.3830(2)	1.07(8)
H (×1/3)	0.3110(9)	0.3110(9)	0.3509(5)	2.1(4)

Table 2 Important derived distances (Å) and angles (°) for $Ca_8[AlGaSiO_6]_4(OH)_8$

Distance		Angle	
Al/Ga/Si–O × 4	1.739(1)	O–Ga/Si/Al–O	110.3(1)
Ca–O × 3	2.440(1)	O–Ga/Si/Al–O × 2	109.6(1)
Ca–O(H) × 4	2.328(1)	Ga/Si/Al–O–Ga/Si/Al	128.8(1)
O–H × 1	0.944(1)		

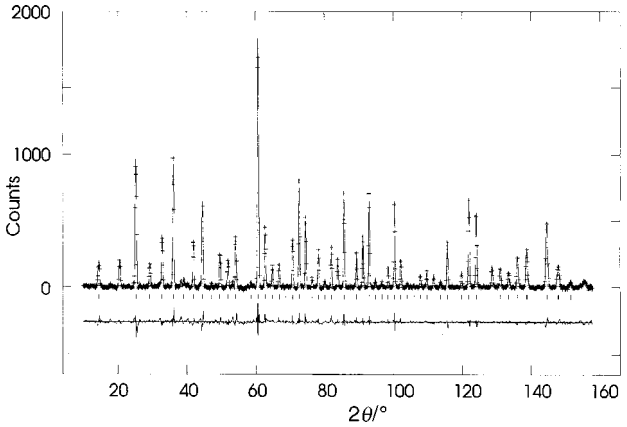

Fig. 3 Final fit achieved to the powder neutron diffraction profile of $Ca_8[Ga_2SiO_6]_4(OH)_8$. Upper continuous line calculated profile, crosses are the experimental points and the lower continuous line is the difference. Tick marks show reflection positions.

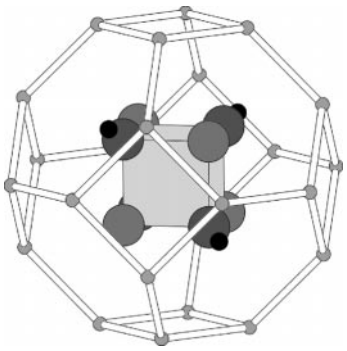

Fig. 4 The $Ca_8[AlGaSiO_6]_4(OH)_8$ structure showing the framework as disordered, directly linked tetrahedral sites and the calcium and hydroxide ions as a cubic $Ca_4(OH)_4$ block.

of most interest in this material is the framework, where gallium, silicon and aluminium all seem to be disordered over the tetrahedral sites. The cell parameter, $a = 8.88114(6)$ Å, the T–O bond length, 1.739(1) Å, and the T–O–T bond angle, 128.8(1)°, all have values intermediate between those of gallobicchulite and bicchulite.[10,11] This would confirm that in terms of the long-range structure these species are disordered. However, a recent detailed analysis of the bicchulite structure using EXAFS as well as diffraction methods shows that locally the trivalent and tetravalent cations are in fact ordered in agreement with Lowenstein's rule. It is likely that aluminium gallium bicchulite has a similar local ordering, which also minimises the number of contacts between tetrahedra containing trivalent metal ions. Of specific interest in this material will be whether individual Al–O–Al, Al–O–Ga or Ga–O–Ga contacts are also minimised; further work using local structure techniques such as EXAFS and MASNMR on this unique material is planned.

The Li–Cu–N system. Li_3N is the only known alkali metal nitride and has a unique structure.[14] Further, the structure contains small levels of lithium vacancies, which gives rise to Li^+ fast ion conductivity and so Li_3N promises much as a battery material. The structure and properties of Li_3N have been extensively investigated. As the structure contains two distinct Li^+ sites, the first within graphitic type sheets and the second between these layers (see Fig. 5), one aim has been to replace the lithium between the $[Li_2N]$ layers with other metals to modify the structure and physical properties of the material. Here, we report studies into replacing the lithium with copper by synthesis under high-pressure nitrogen. Previous work

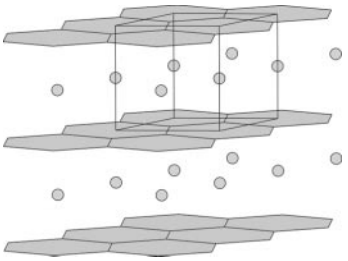

Fig. 5 The $Li_{3-x}Cu_xN$ structure shown as hexagonal layers of Li_2N^- connected by lithium/copper ions.

under 1 bar of nitrogen[15] indicated a limit on the level of copper that can be incorporated at $Li_{2.7}Cu_{0.3}N$.

$Li_{3-x}Cu_xN$ samples were synthesised by the combination of Li_3N (Aldrich) and copper powder (Aldrich) under high-pressure dry electronic grade nitrogen (BOC). The apparatus was described earlier. Initially, the aim was to achieve complete substitution of the interlayer lithium with copper and so Li_2CuN was the target material. Preparations were carried out under 200 bar nitrogen at 700 °C for 16 h with a cooling rate of 4 °C min^{-1}. Preliminary characterisation of the products was done using powder X-ray diffraction. This showed the presence of unreacted copper in the product, as well as $Li_{3-x}Cu_xN$; the successful incorporation of copper was demonstrated by significant lattice parameter changes from those of Li_3N. Further annealing failed to remove the copper and so dilution of the product with Li_3N, with intermediate annealing under the conditions described above, was carried out until the powder diffraction pattern no longer contained any copper peaks. This revealed that the maximum copper substitution was around $x = 0.55$. Two new experiments were carried out where $x = 0.5$ and 0.6. The first was found to contain no unreacted copper and the second a very small amount of copper metal. It was decided to characterise the $x = 0.6$ material as this contained the maximum copper substituted product.

Powder X-ray diffraction data on $Li_{2.4}Cu_{0.6}N$ were collected using a Siemens D5000 diffractometer (Cu-Kα_1). Powder neutron diffraction data were obtained using the high flux, medium resolution diffractometer, POLARIS, at the Rutherford Appleton Laboratory, Didcot, Oxon. Rietveld refinement was carried out using GSAS[13] on the powder neutron data set; these data were chosen owing to the difficulty of distinguishing lithium and a vacancy using powder X-ray diffraction data. The starting model was that of Li_3N with lattice parameters calculated by the CELL program from the powder X-ray data. The unreacted copper and a small amount of lithium oxide were modeled as second and third phases. The refinement converged smoothly to give the atomic data in Table 3 (only the ternary phase is presented) and the profile in Fig. 6. No evidence of copper substitution into the $[Li_2N]$ layers was apparent from the refinement but substantial lithium vacancies were found in this portion of the structure.

In comparison with the parent Li_3N phase, $Li_{2.4}Cu_{0.6}N$ shows marked differences in lattice parameters with a large contraction along c resulting from replacement of lithium by copper in the sites connecting the layers. The average Li/Cu–N bond length is reduced from 1.938 Å in lithium nitride to

Table 3 Final refined atomic parameters for $Li_{2.45}Cu_{0.55}N$ (space group *P6/mmm*)

Atom	x	y	z	Occupancy	$U_i/U_e \times 100/Å^2$
N	0	0	0	1.0	0.83(2)
Li(1)	$\frac{1}{3}$	$\frac{2}{3}$	0	0.857(14)	2.81(8)
Li(2)	0	0	$\frac{1}{2}$	0.481(3)	0.52(3)
Cu	0	0	$\frac{1}{2}$	0.519(3)	0.52(3)

Lattice parameters: $a = 3.67922(3)$ Å, $c = 3.75095(4)$ Å.

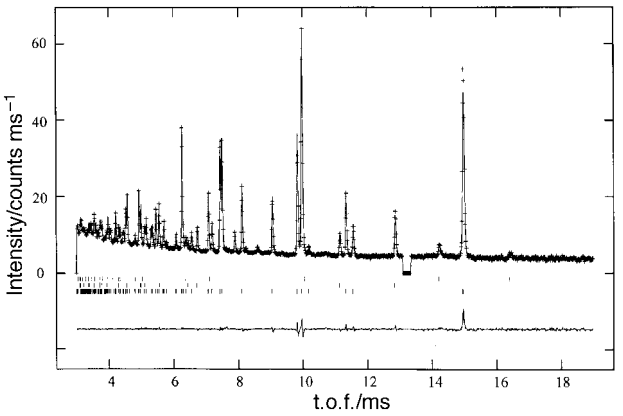

Fig. 6 Final fit achieved to the powder neutron diffraction profile of $Li_{2.4}Cu_{0.6}N$. Upper continuous line calculated profile, crosses are the experimental points and the lower continuous line is the difference. Tick marks show reflection positions.

1.875 Å in $Li_{2.4}Cu_{0.6}N$. However, the *a* lattice parameter actually increases slightly, presumably as a result of the significant number of lithium vacancies in the 'Li_2N' layer. These changes in bond lengths and the compound stoichiometry probably indicate that the copper enters the structure, at least partially, in a higher oxidation state than Cu^+.

Nickel doped 247 compounds. The material $Y_2Ba_4Cu_7O_{14+\delta}$ (247) is a well known superconducting phase with a structure that can be considered as a 1 : 1 intergrowth of the $YBa_2Cu_3O_7$ (123) and $YBa_2Cu_4O_8$ (124) phases.[8] The effect of doping into the 123 structure has been studied in detail where it normally results in the partial replacement of copper in the CuO_2 layers, rapidly destroying the superconducting properties. However, replacement of the copper site that connects the CuO_2 layers does not affect the superconducting properties to the same extent and superconducting materials such as $YSr_2Cu_2GaO_8$ are well characterised. In the 247 structure a range of four possible sites exist for replacing copper as shown in Fig. 7. In order to investigate which sites are substituted in this structure a series of compounds of the type $Y_2Ba_4Cu_{7-x}Ni_xO_{14+\delta}$ have been synthesised and studied using neutron diffraction. As pure crystalline 247 material can only be made under high-pressure oxygen the apparatus described earlier was used to generate these materials.

Stoichiometries representative of the required phase in the $Y_2Ba_4Cu_{7-x}Ni_xO_{14+\delta}$ (247) system, $x=0$, 0.2, 0.4, 0.6, 0.8, 1.0, were prepared from high purity Y_2O_3, $BaCO_3$, CuO and NiO. These mixtures were then fired in air at 920 °C and samples were reground periodically during a reaction time of four days. Products were examined using powder X-ray diffraction and found to consist of a mixture of two phases: CuO and a nickel-doped Ln123-type phase. There appeared to be no sign of unreacted nickel oxide by X-ray diffraction indicating that the nickel was present in the Ln123-type phase. This intimate mixture was then subjected to a high-pressure oxygen annealing treatment. The sample was loaded into a gold crucible and heated at 1020 °C in 70 atm flowing oxygen gas for a period of 12 h.[10] A cooling rate of 3 °C min^{-1} was used and this process was repeated to achieve full reaction. Powder X-ray diffraction confirmed the presence of a Ln247-type phase and the apparent absence of either nickel or copper oxide. Cell parameters were calculated for all samples and the variation in *c* is shown in Fig. 8 clearly showing a marked reduction; this is accompanied by a slight reduction in the orthorhombic distortion. Thermogravimetric analysis of the products was undertaken on a Stanton Redcroft TGA1500 thermal balance by heating under 5% H_2 in N_2. Results showed that the oxygen level in the series of materials $Y_2Ba_4Cu_{7-x}Ni_xO_{14+\delta}$ increased slightly from 15.0 to 15.1 as the nickel content rises and this may account, in part, for the slight reduction in orthorhombicity.

Full structural characterisation was again carried out using powder neutron diffraction; the large contrast in copper and nickel scattering lengths should allow the determination of the nickel distribution over the four possible copper sites. To this end, data from samples of nominal compositions $Y_2Ba_4Cu_{6.8}Ni_{0.2}O_{14+\delta}$, $Y_2Ba_4Cu_{6.5}Ni_{0.5}O_{14+\delta}$ and $Y_2Ba_4Cu_{6.0}Ni_{1.0}O_{14+\delta}$ were collected on the D2B powder neutron diffractometer at Institut Laue-Langevin in Grenoble, France. Samples were mounted in thin-walled vanadium cans and data were obtained using a wavelength of 1.5943 Å at room temperature; a step size of 0.05° 2θ was used. Rietveld refinement of the data using the program GSAS[13] proceeded with the refinement of cell parameters, atomic positions and isotropic temperature factors. Site occupancies of nickel and copper, distributed over the four different B cation type sites within the Ln247 structure as shown in Fig. 7, and constrained to fit the compound stoichiometry, were refined in order to ascertain the location of the nickel dopant within the structure. Full detail of this analysis will be published elsewhere[16] but for the highest dopant levels nickel was located, unequivocally the two square pyramidal sites, Fig. 7.

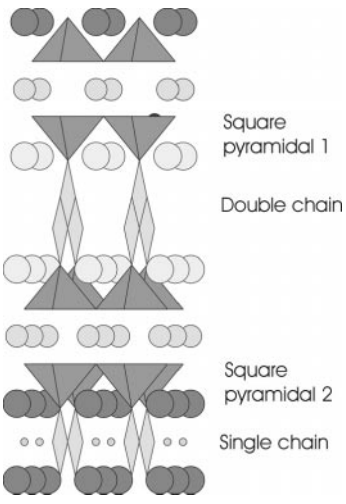

Fig. 7 $Y_2Ba_4Cu_{7-x}Ni_xO_{14+\delta}$ ($x=0.2$, 0.4, 0.6, 0.8, 1.0) showing the different copper sites on to which nickel may be doped.

Discussion

The majority of synthesis work in materials chemistry is undertaken at ambient pressure, however, such a restricted synthesis regime strongly limits the chemistry in terms of phases that are stable. In this paper three different methods

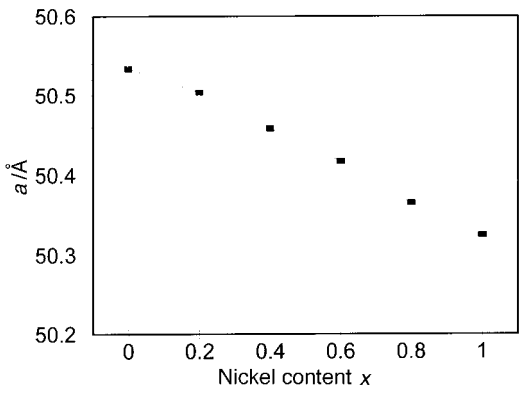

Fig. 8 Variation of the *c* cell parameter in the system $Y_2Ba_4Cu_{7-x}Ni_xO_{14+\delta}$ as a function of *x*.

of achieving reaction under high pressure are described and in each case the range and stoichiometry of materials that can be obtained is significantly augmented. For example, frameworks with linked Al–O–Ga tetrahedra are unknown through synthesis at ambient and near ambient pressures though they can be generated under high-pressure hydrothermal conditions as shown in this article. At the lower temperatures normally employed in aluminosilicate framework synthesis, thermodynamic and kinetic factors preclude the formation of linkages between tetrahedra containing trivalent ions in aqueous media. The potential for generating new materials, with unusual chemical combinations, under these high-pressure hydrothermal conditions is probably enormous.

The range of stability of various oxidation states may also be increased through high pressures. For example oxygen at 1 kbar provides, at least, an additional oxygen chemical potential of 70 kJ mol^{-1}. Under these conditions it is possible to stabilise high oxidation states of the late transition metals such as Ni^{3+}, Co^{3+} and Cu^{3+} in combination with less electropositive elements such as lanthanides and lithium. This behaviour is very apparent in cuprate superconductor chemistry with a number of phases such as 124, 247 and $YSr_2Cu_2GaO_8$ requiring high-pressure oxygen for their formation as highly crystalline materials. In this paper it has been possible to generate new nickel doped 247 phases by reaction under high-pressure oxygen. Considerable levels of nickel may be introduced into these materials under these conditions with facile substitution at one of the square pyramidal sites within the structure. Synthesis under high pressure has played a major part in the development of superconducting cuprate chemistry over the past 5 years producing a number of very complex phases which include compounds such as 247, the multi-copper layer mercury superconductors and the anion containing systems. The synthesis of such complex structures under high pressures has been limited to cuprate chemistry but there is no reason why such high-pressure techniques should not be applied to the formation of complex structures for other transition metals.

The area of nitride chemistry has also developed rapidly over the past decade though most of this work has again been limited to ambient pressure studies. High-pressure nitrogen should extend the range of nitride phases that can be synthesised, as demonstrated in this article, and in our recent report of a new calcium gold nitride, Ca_2AuN.[17]

We thank the EPSRC for grants which have supported work in the various areas described in this article and for the provision of beam time at the Rutherford-Appleton Laboratory (ISIS) and the ILL.

References

1 Y. Matsui, T. Kawashima and E. Takayama-Muromachi, *Physica C*, 1994, **235–240**, 166.
2 E. Ito, *Earth Planet Sci. Lett.*, 1978, **38**, 443.
3 J. Beille, B. Chevalier, G. Demazeau, F. Deslandes, J. Etourneau, O. Laborde, C. Michel, P. Lejay, J. Provost, B. Raveau, A. Sulpice, J. L. Tholence and R. Tournier, *Physica B*, 1987, **146**, 307.
4 M. Ajomand and D. Machin, *J. Chem. Soc., Dalton Trans.*, 1975, 1055.
5 B. Cleaver and D. B. Currie, *High Temp. High Press.*, 1990, **22**, 623.
6 M. T. Weller, D. R. Lines and D. B. Currie. *J.Chem Soc., Dalton Trans.*, 1991, 3137.
7 D. B. Currie and M. T. Weller, *Physica C*, 1993, **214**, 204.
8 D. B. Currie and M. T. Weller, *Physica C*, 1993, **216**, 140.
9 S. E. Dann, P. J. Mead and M. T. Weller, *Inorg. Chem.*, 1996, **35**, 1427.
10 S. E. Dann, P. J.M ead and M. T. Weller, *Angew. Chem.*, *Int. Ed. Engl.*, 1995, **34**, 2414.
11 N. Binsted, M. J. Pack, S. E. Dann and M. T. Weller, *Acta Crystallogr., Sect. B*, in press.
12 J. Skibsted, P. Norby, H. Bildsoe and H. J. Jakobsen, *Solid State NMR*, 1995, **5**, 239.
13 A. C. Larson and R. B. von Dreele, GSAS, Los Alamos, NM, 1990.
14 A. Rabenau and H. Schulz, *J. Less Common Met.*, 1976, **50**, 155.
15 W. Sachsze and R. Juza, *Z. Anorg. Allg. Chem.*, 1949, **259**, 278.
16 D. B. Currie and M. T. Weller, *Physica C297*, 1998, 95.
17 P. F. Henry and M. T. Weller, *Angew. Chem.*, in press.

Paper 8/04641G